NUMERICAL REQUIREMENTS IN THE CALCULATION OF FLOW OVER BODIES OF REVOLUTION AT INCIDENCE

Tuncer Cebeci, A.A. Khattab and S.M. Schimke
Aerodynamics Research and Technology
Douglas Aircraft Company, Long Beach, California

Abstract

Uncertainty in the accuracy of the calculated separation line of flows over bodies of revolution at incidence prompted this examination of numerical features of the solution of the corresponding three-dimensional boundary layers. The requirements of different marching directions and of numerical grids are examined. It is shown that the direction of marching is unimportant provided an intelligent numerical scheme, such as the Characteristic Box scheme, is used in regions where negative crossflow is present. This implies that the ratio of space to time steps must satisfy a stability requirement and tests are conducted to determine the limitations and the consequences of exceeding them.

Introduction

Solutions of the steady laminar and turbulent boundary-layer equations for two-dimensional flows can be obtained for a wide range of flow conditions with efficient and accurate numerical methods and with novel interaction procedures as described by Cebeci, Stewartson and Whitelaw[1] and Cebeci and Whitelaw[2]. Corresponding calculation methods for three-dimensional flows with separation are, however, in their infancy due partly to difficulties associated with solving the three-dimensional boundary-layer equations, even for a given pressure distribution, and to the lack of a properly formulated interactive scheme. In this paper, we address the former problem and describe an accurate numerical procedure and its application to turbulent flow over a prolate spheroid, for which analytical expressions are available for the inviscid pressure distribution. In addition, the experiments of Meier and Kreplin[3], Ramprian, Patel and Choi[4], and Meier et al.[5,6] can be used to assist the evaluation of the numerical procedure.

We will consider the arrangements of Meier et al.[5] who measured flow and surface characteristics around a spheroid which has major and minor axes of 2.4m and 0.4m, respectively, for freestream velocities of 45 and 55 m/s in the 3m x 3m wind tunnel of the DFVLR, Göttingen, at an angle of attack of 10 degrees and with natural and imposed transition. Calculations of the flows with natural transition have been reported by Patel and Baek[7] with their ADI scheme and a two-equation turbulence (k-ε) model, and by Cebeci[8] with Keller's Box scheme and the Cebeci-Smith algebraic eddy-viscosity formulation. Even though the solution procedures of Patel and Baek, and Cebeci et al. differed from each other in their numerical and turbulence-model assumptions, the computed results were practically the same and in close agreement with the measurements. Separation occurred in the downstream region but the accuracy with which the separation locations were calculated was not pursued since the assumed inviscid-pressure distribution differed from the measured pressure distribution in the regions approaching flow separation.

The subsequent calculations by Meier and Cebeci[9] for the same geometry and imposed transition also revealed good agreement with experiment for most parts of the flow but oscillations were observed for $x > 0.44$ and the solutions broke down at $x = 0.615$. Oscillations and breakdown of this type are frequently associated with separation but separation was not observed in the experiments.

Numerical features of the calculation of these flows are considered in this paper which shows that the results can depend on the manner in which the calculations proceed from one line of symmetry to the other: this problem is examined in the following section. The third section of the paper examines the dependence of solutions on the numerical mesh and confirms that a stability criterion, such as that of Courant, Friedrichs and Lewy (CFL)[10] must be considered in solving the three-dimensional equations. The paper ends with a statement of the more important conclusions.

Comments on the Solution Procedure

The solution of the three-dimensional boundary-layer equations requires initial conditions along two intersecting planes which correspond to the (x,y) and (ϕ,y) planes in the case of a body of revolution at incidence. Those on the (ϕ,y) plane can be obtained from equations which take into account the symmetry of the flow conditions and those on the (x,y) plane depend on the coordinate system and require special procedures. With a body-oriented coordinate system, the geometric parameters have a singularity at the nose and this can be removed by transformations so that the boundary-layer equations can be solved to generate initial conditions in the (x,y) plane as discussed by Cebeci, Khattab and Stewartson[11]. Here we shall adopt this procedure, assume that the initial conditions on the (x,y) plane are generated at $x = x_0$ and discuss the solution of the boundary-layer equations downstream of this plane.

The flow on a body of revolution at incidence usually has one plane of symmetry but two initial (ϕ,y) planes, one on the windward side and the other on the leeward side. The solution of the full three-dimensional boundary-layer equations can be obtained at $x = x_0$ with initial conditions generated on either line of symmetry and continued in the circumferential direction. The marching procedure raises the question of a preferred direction and its role in the development of the numerical procedure. To elaborate on this point further, consider laminar flow over a prolate spheroid at $\alpha = 6°$, for which Figure 1 shows the separation lines and the line on which circumferential skin-friction coefficient c_{f_ϕ} is zero.[12] In the region upstream of the line of zero c_{f_ϕ} (Region A) all u and w velocities are positive, in the region between this line and the two separation lines (Region B), u is positive and w is negative near the surface, and in the region downstream of the separation lines (Region C) u and w are negative

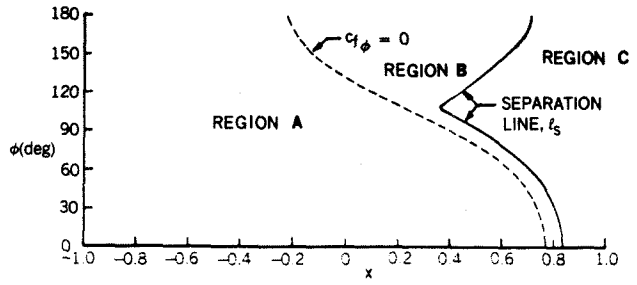

Figure 1. Definition of flow regions on a prolate spheroid at incidence, (laminar flow, $\alpha = 6°$).

near the surface and positive away from the surface.

The boundary-layer calculations can be performed in Regions A and B for a prescribed pressure distribution because the flow is attached and solutions can be obtained with initial conditions started on either line of symmetry. In Region A, however, it is logical to initiate the calculations on the windward line because the crossflow velocity is in the marching direction whereas the crossflow direction will be opposite to the marching direction if they originate on the leeward line. In the former case, the solutions can be obtained by a standard numerical procedure such as those of Crank and Nicolson[13] or Keller[14] and, in the latter case, a special numerical method is required to march in the direction opposite to that of the flow. Since the accuracy of the standard procedure is well established, results obtained for region A can be used to establish the accuracy of the special procedure which is required to calculate the negative crossflow velocities of region B.

Numerical Method and Stability Requirements

In the present study we use the numerical methods of Keller with the Standard Box (SB) scheme in regions of positive crossflow velocity and the Characteristic Box (CB) scheme in the presence of negative crossflow velocity. A description of the latter scheme has been given by Keller[15] and Cebeci[16,17] for unsteady flows, and by Cebeci et al.[12] and Cebeci[17] for three-dimensional flows. In this second case, the accuracy of the solutions is strongly dependent on the choice of the net in the circumferential and streamwise directions and this is examined further with the net shown in Figure 2 at a given distance y from the surface and with the assumption that the solutions originate on the leeward line of symmetry; the symbol x denotes the known solution and the symbol o denotes the desired solution. The backward characteristic from point P is in the local streamline direction and intersects the x_{i-1} line at E when there is a positive crossflow velocity rather than at F when the crossflow velocity is negative. Since the CB scheme computes the region EFP, which is known as the domain of dependence of point P, it allows the "correct" information to reach point P from region EFP. It is important that the domain of stable computations can be determined a priori and this can be achieved by determining the ratio $\beta(\equiv \Delta\phi_1/\Delta\phi)$ and requiring that it remains small during the calculations: we shall refer to this requirement as the CFL-like condition.

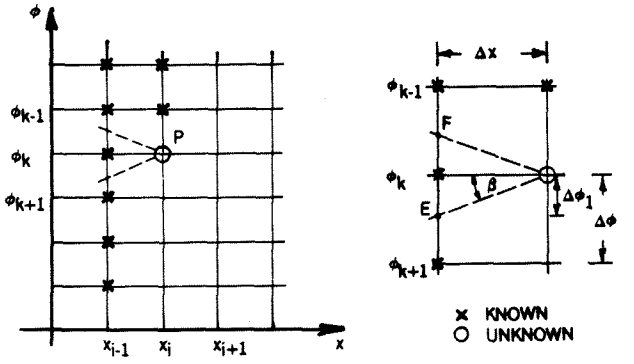

Figure 2. Finite-difference net for the Characteristic Box scheme.

The initial conditions in the (ϕ,y) plane are generated by the procedure[12] at $x_0 = -0.90$ for laminar flow and calculations further downstream were obtained for specified Δx-step lengths with transition specified in accord with the experiments at $x = -0.56$. Region A extended to $x = -0.72$ where the circumferential skin friction first became zero and region B from $x = -0.72$ to -0.48 with negative crossflow appearing near the leeward line of symmetry. The circumferential velocity w was positive throughout the region $-0.48 \leq x \leq -0.03$, as in region A, due to the assumption that turbulent flow began at $x = -0.56$. However, for $x \geq -0.03$, the negative crossflow reappeared on the leeward line of symmetry and increased in size with increasing x.

Two sets of calculations were performed, the first in region A for $-0.9 \leq x \leq -0.72$, and the second in the region defined by $x > -0.72$. In each region, uniform 2.5° increments in ϕ were used with variable x-step lengths and with different marching procedures.

The calculations in region A made use of the SB scheme starting on the windward line of symmetry and marching towards the leeward side with uniform Δx-increments of 0.03. They were also performed with the CB scheme from the leeward line of symmetry marching in the windward direction and using the same grid: the results showed that the CFL-like parameter increased rapidly with subsequent breakdown of the solutions. Smaller uniform step-lengths in the x-direction equal to 0.01 and 0.005, allowed the calculations to proceed without breakdown and with the expected lower values of the CFL parameter.

A sample of the results is shown on Table 1 and in Figure 3 for $x = -0.72$. We note that the CB solutions for the streamwise wall shear parameter $f''(0)$ break down around $\phi \approx 130°$ where the same grid ($\Delta x = 0.03$) is used in the SB scheme and, even though the CB solutions from the leeward line of symmetry agree with the SB solutions from the windward side, they diverge progressively with increasing ϕ. The parameter β, shown in Figure 3, increases rapidly with the coarse grid ($\Delta x = 0.03$). With the smaller Δx-steps ($\equiv 0.01$, 0.005), however, the two solutions are in good agreement for all values of ϕ with no breakdown and considerable reduction in β. These results suggest that with the proper grid, the accuracy of the CB scheme is almost identical

Table 1. Comparison of Streamwise Wall Shear Parameter f"(0) Computed with SB and CB Schemes at x = -0.72

	Standard Box (SB)		Characteristic Box (CB)		
φ°	Δx = 0.03	Δx = 0.005	Δx = 0.03	Δx = 0.01	Δx = 0.005
0	0.7294	0.7290		0.7293	0.7290
20	0.7231	0.7227		0.7239	0.7232
40	0.7028	0.7024		0.7034	0.7028
60	0.6671	0.6669		0.6673	0.6669
80	0.6145	0.6141		0.6141	0.6139
100	0.5439	0.5433		0.5427	0.5425
120	0.4554	0.4554		0.4543	0.4541
130	0.4073	0.4078		0.4054	0.4053
135	0.3865	0.3845	0.4542	0.3812	0.3815
140	0.3630	0.3633	0.3448	0.3595	0.3598
145	0.3468	0.3452	0.3441	0.3429	0.3427
150	0.3326	0.3337	0.3285	0.3328	0.3320
160	0.3264	0.3282	0.3269	0.3304	0.3289
170	0.3349	0.3371	0.3351	0.3383	0.3360
180	0.3444	0.3443	0.3444	0.3450	0.3443

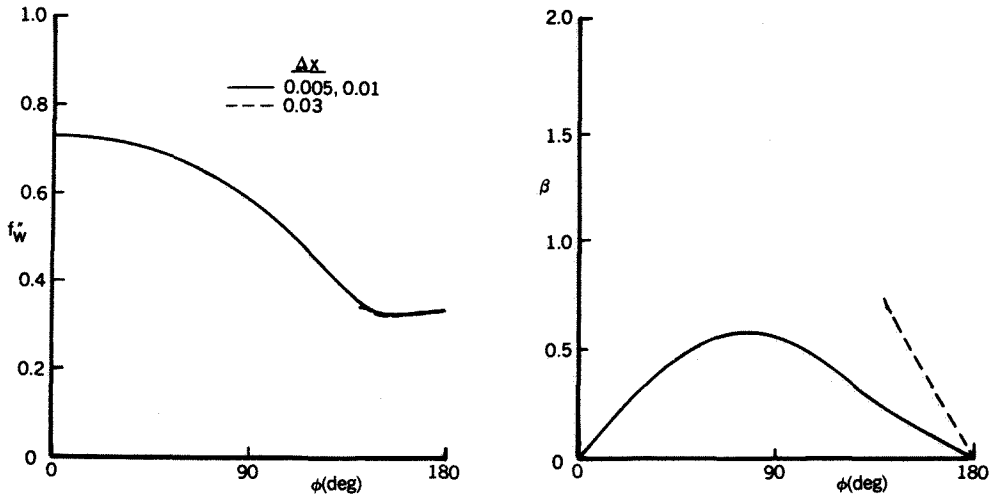

Figure 3. Variation of skin-friction parameter and β with circumferential distance at x = -0.72.

to that of the SB scheme which is second order. The CFL β is a measure of the numerical accuracy.

Figure 4 permits comparison between the solutions of the CB scheme with two different Δx-spacings at x = -0.78. As can be seen, the wall shear parameter f"(0) exhibits oscillations with relatively high values of β prior to the breakdown of the coarse-grid solutions at x = -0.72. However, with smaller Δx-spacing these oscillations upstream of x = -0.72 disappear and the solutions have much smaller values of β.

The calculations for x > -0.72, made use of three separate x-steps: a constant value of Δx = 0.03, a step variation with Δx = 0.01 in the range $-0.72 \leq x \leq -0.48$, 0.03 in the range $-0.48 \leq x \leq -0.03$ and 0.01 for x > -0.03. The third set of calculations made use of the same x-steps as in the second set except that Δx was decreased to 0.005 from 0.01 for $0.40 \leq x \leq 1$. The calculations using the first uniform grid in the x-direction (Δx = 0.03) indicated breakdown of the solutions at x = 0.69 whereas those with two other spacings in x did not. As in region A, two separate marching procedures were used to compute the flow. In the first, solutions were initiated on the windward line of symmetry and the calculations were performed by marching from φ = 0 to 180°. In regions of positive and negative circumferential flow velocity, w, the calculations made use of the SB and CB schemes, respectively. In the second case, the CB scheme was used with solutions initiated on the leeward line of symmetry and marching towards the windward line of symmetry in regions of negative w; the rest of the flow was computed by the SB scheme with solutions initiated on the windward line of symmetry. Comparison of the results of the two procedures showed, however, that the predictions in both cases were essentially the same and that there was no preferred direction of marching. With the fixed Δx-spacing, the solutions broke down with solutions originating from both lines of symmetry.

Figure 5 shows the computed results at x = 0.46 which corresponds to x/2a = 0.73 and Figure 6 those at x = 0.65 corresponding to x/2a = 0.825. The

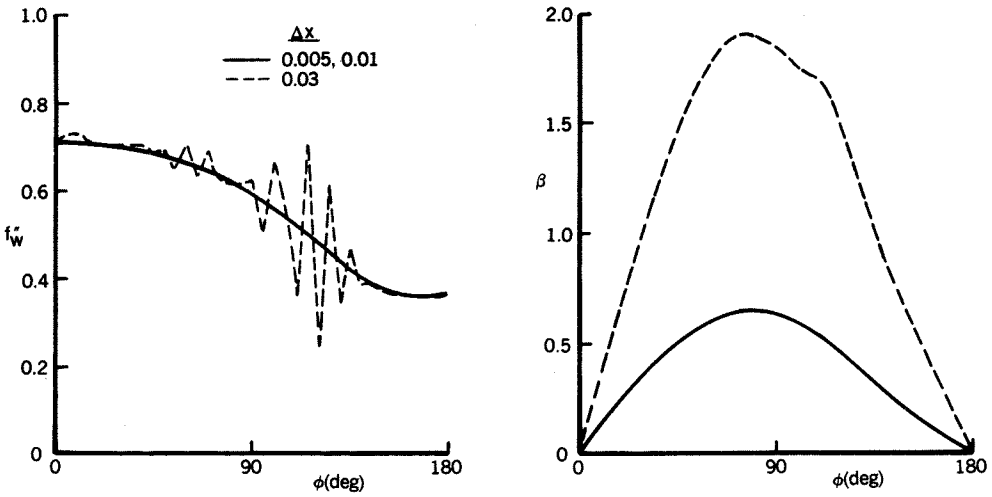

Figure 4. Variation of skin-friction parameter and β with circumferential distance at x = -0.78.

results at x = 0.46 may also be compared with experimental data and the effect of the grid evaluated.

Figure 5a shows that the coarse grid (Δx = 0.03) predicts the peak in the measured displacement thickness whereas, those computed with the two fine grids (Δx = 0.01 and 0.005) do not, with relatively small differences between the results obtained with the two fine grids. The computed crossflow angles, designated by γ, are in better accord with the measurements when computed with the fine grids, as shown by Fig. 5b. Both fine grid calculations indicate a maximum crossflow angle of around 10, in agreement with the measured value, and in contrast with the coarse grid results of 12.

Figure 5c allows comparison between the dimensionless wall shear-stress parameters f"(0) and g"(0), in the x and φ directions, respectively, computed with three Δx-spacings. Both parameters are influenced by the Δx-spacing in the same way and the corresponding variations of β, Fig. 5d, show the expected decrease with Δx. The results obtained in region A suggested that the value of β should be less than around 0.4 and those of Fig. 5d support this conclusion. The discrepancies between the fine-grid calculations of Fig. 5a and 5b and the measurements occur in spite of this support for the numerical accuracy.

Figure 6a and 6b show the crossflow angles and β-distributions at x = 0.65, a distance considerably downstream from that of the results of Fig. 5, again with three values of Δx spacing. The crossflow angles with Δx of 0.03 are clearly in error and this is supported by the very large corresponding values of β: an attempt to extend this calculation further downstream led to breakdown at x = 0.845. As with Fig. 5, there is a monotonic variation of β with Δx spacing except in a small region of φ where the coarse-grid calculation oscillates. The fine-grid calculation leads to values of β which are less than 0.4 and this, consistent with the previous results, suggests that this solution is of acceptable accuracy.

Concluding Remarks

Two main conclusions stem from the previous pages. They are concerned with the direction of calculations in regions of negative crossflow and with the need to determine a criterion which will guide the choice of mesh and ensure acceptable numerical accuracy.

A special numerical scheme is required to allow calculations to march against the flow direction and the Characteristic Box scheme has been used successfully for this purpose. The accuracy of numerical schemes such as that based on Keller's Standard Box, is well established and these can be used in regions where flow reversals do not occur in the circumferential direction to establish the accuracy of the special numerical schemes used to calculate in the direction opposite to the flow.

The calculations performed for flow around a body of revolution at incidence show that a parameter in the Characteristic Box scheme, defined as $\beta \equiv \Delta\phi_1/\Delta\phi$, can be used as a measure of numerical accuracy. The results suggest that this parameter, which is related to the location where the backward characteristic intersects the previous constant x-line, must not exceed around 0.4.

Acknowledgment: This research was supported under Air Force Office of Scientific Research contract F49620-84-C-0007.

REFERENCES

1. Cebeci, T., Stewartson, K. and Whitelaw, J.H.: Calculation of Two-Dimensional Flows Past Airfoils. In Numerical and Physical Aspects of Aerodynamic Flows II (T. Cebeci, Ed.), 1-40, Springer-Verlag, 1984.

2. Cebeci, T. and Whitelaw, J.H.: Calculation Methods for Aerodynamic Flows - A Review. In Numerical and Physical Aspects of Aerodynamic Flows III (T. Cebeci, Ed.) Springer-Verlag, 1986.

3. Meier, H.U. and Kreplin, H.P.: Experimental Investigation of the Boundary-Layer Transition and Separation on a Body of Revolution. Zeitschrift f. Flugwiss Weltraumforsch 4, 65, 1980, 1980.

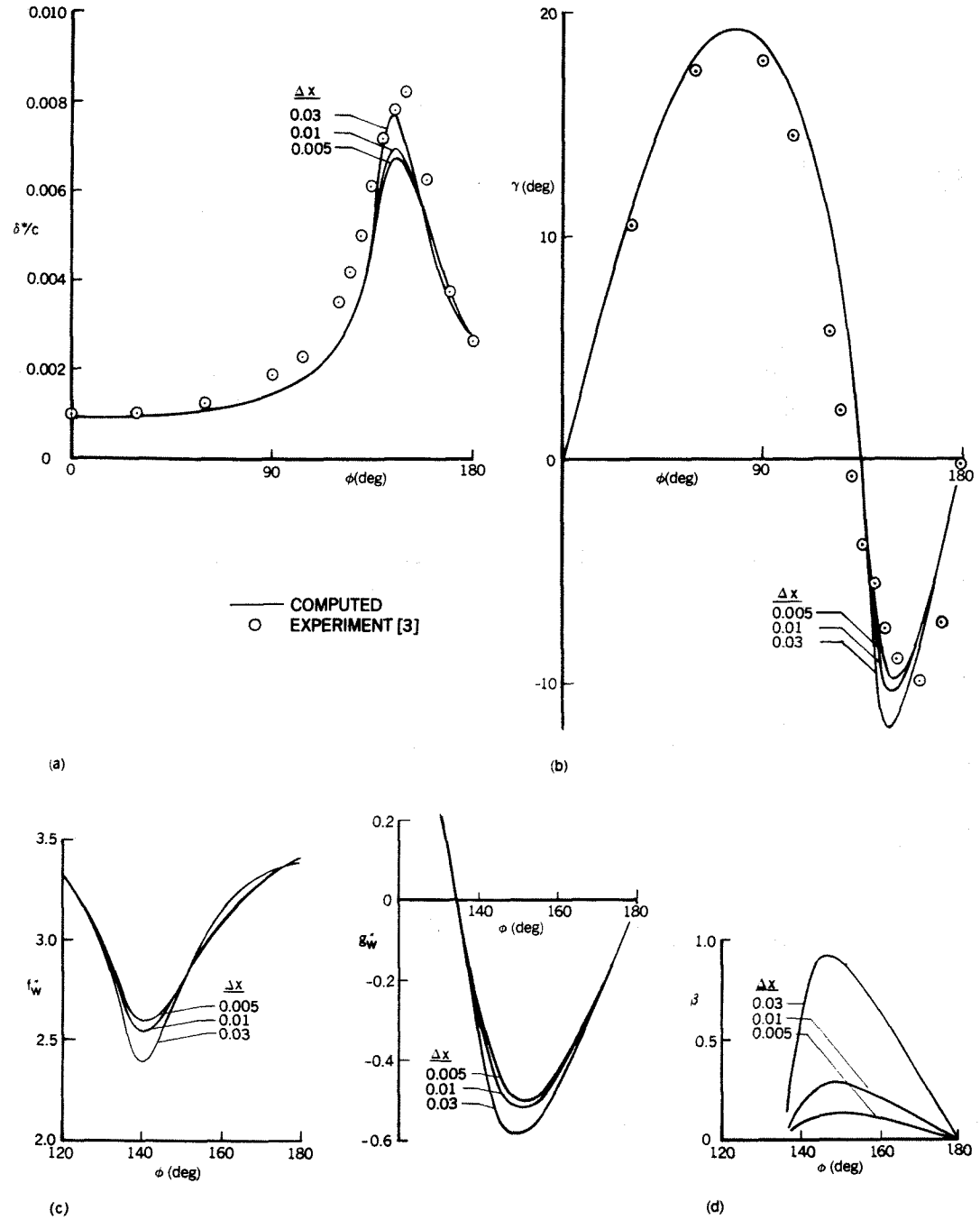

Figure 5. Variations with circumferential distance at x/2a = 0.73 of (a) displacement thickness, (b) crossflow angle, (c) dimensionless wall shear-stress parameters and (d) β parameter.

4. Ramprian, B.R., Patel, V.C. and Choi, D.H.: Mean-Flow Measurements in the Three-Dimensional Boundary Layer Over a Body of Revolution at Incidence. J. Fluid Mech. 103, 479, 1981.

5. Meier, H.U., Kreplin, H.-P., Landhäußer, A. and Baumgarten, D.: Mean Velocity Distributions in Three-Dimensional Boundary Layers Developing on a 1:6 Prolate Spheroid with Natural Transition (α = 10°, U_∞ = 45 m/s, Cross Sections: x/2a = 0.56, 0.64 and 0.73) - Data Report. DFVLR, IB 222-84 A 10, 1984.

6. Meier, H.U., Kreplin, H.-P., Landhäußer, A. and Baumgarten, D.: Mean Velocity Distributions in Three-Dimensional Boundary Layers Developing on a 1:6 Prolate Spheroid with Artificial Transition (α = 10°, U_∞ = 55 m/s, Cross Sections: x/2a = 0.48, 0.56, 0.64 and 0.73) - Data Report. DFVLR, IB 222-84 A 11, 1984.

7. Patel, V.C. and Baek, J.H.: Boundary-Layers and Separation on a Spheroid at Incidence. AIAA J. 23, 55-63, 1985.

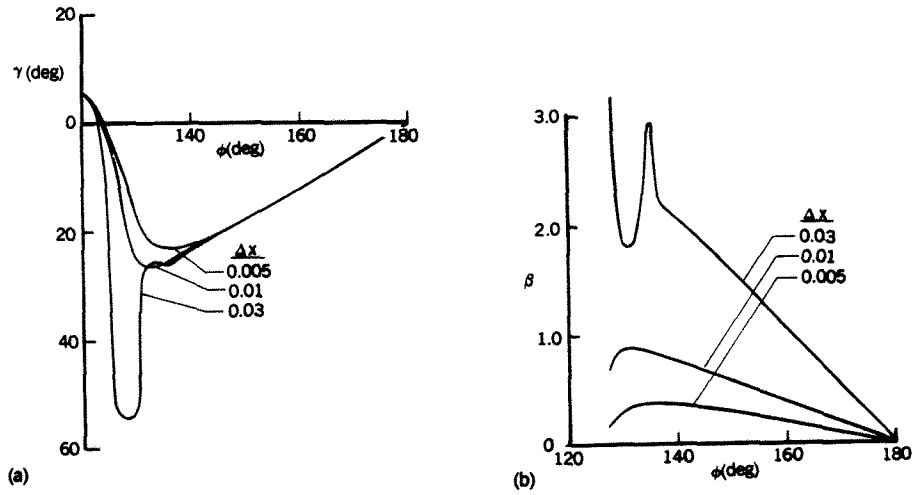

Figure 6. Variations with circumferential distance at x/2a = 0.83 of (a) crossflow angles and (b) β parameter.

8. Cebeci, T.: Problems and Opportunities with Three-Dimensional Boundary Layers. AGARD Rept. No. 719, Three-Dimensional Boundary Layers, 1984.

9. Meier, H.U. and Cebeci, T.: Flow Characteristics of a Body of Revolution at Incidence. Proc. of 3rd Symposium on Numerical and Physical Aspects of Aerodynamic Flows. California State University, Long Beach, 1985.

10. Isaacson, E. and Keller, H.B.: Analysis of Numerical Methods, John Wiley, New York, 1966.

11. Cebeci, T., Khattab, A.A. and Stewartson, K.: On Nose Separation. J. Fluid Mech. 97, 435, 1980.

12. Cebeci, T., Khattab, A.A. and Stewartson, K.: Three-Dimensional Laminar Boundary Layers and the Ok of Accessibility. J. Fluid Mech. 107, 57, 1981.

13. Crank, J. and Nicolson, P.: A Practical Method of Numerical Evaluation of Solutions of Partial-Differential Equations of the Heat-Conduction Type. Proc. Cambridge Phil. Soc. 43, 50, 1947.

14. Keller, H.B.: Accurate Difference Methods for Two-Point Boundary-Value Problems, SIAM J. Numer. Anal. 11, 305, 1974.

15. Keller, H.B.: Numerical Methods in Boundary-Layer Theory. Ann. Rev. Fluid Mech. 10, 417-433, 1978.

16. Cebeci, T.: Unsteady Boundary Layers with an Intelligent Numerical Scheme. J. Fluid Mech. 163, 129, 1986.